Early Version – Uncorrected



Cannabidiol-Loaded Hyaluronic Acid Hydrogels: Solubilization via β-Cyclodextrin Micelles

Waritorn Srakhao, Phoomipat Boonmapluk, Nontharit Sakda, Teerapol Srichana

DOI: https://dx.doi.org/10.31584/jhsmr.20261500

Received: 12 May 2026

Revised: 13 May 2026

Accepted: 19 May 2026

Published online: 9 November 2026

This paper was from The 8th Current Drug Development International Conference 2026 (May 21-23, 2026).

Please cite this article as: Srakhao W, Boonmapluk P, Sakda N, Srichana T. Cannabidiol-loaded hyaluronic acid hydrogels: solubilization via β-cyclodextrin micelles. J Health Sci Med Res doi: https://dx.doi.org/10.31584/jhsmr.20261500

Early Version — Uncorrected: This accepted manuscript has not been typeset or proofread. Content and formatting may change prior to final publication and should not be regarded as the final Version of Record.

© 2026 JHSMR. Hosted by Prince of Songkla University.

This is an open access article under the CC BY-NC-ND license (https://creativecommons.org/licenses/by-nc-nd/4.0/).

Original Article

Cannabidiol-Loaded Hyaluronic Acid Hydrogels: Solubilization via β-Cyclodextrin Micelles

Waritorn Srakhao, PhD[1,2], Phoomipat Boonmapluk, PharmD[1], Nontharit Sakda, PharmD[1], Teerapol Srichana, PhD[1,3*]

[1] Department of Pharmaceutical Technology, Faculty of Pharmaceutical Sciences, Prince of Songkla University, Songkhla, 90110, Thailand.

[2] Translational Medicine Research Center, Faculty of Medicine, Prince of Songkla University, Songkhla, 90110, Thailand

[3] Drug Delivery System Excellence Center and Department of Pharmaceutical Technology, Faculty of Pharmaceutical Sciences, Prince of Songkla University, Songkhla, 90110

Author

Contact: Waritorn Srakhao

E-mail: waritorn.s@psu.ac.th

ORCID iD: 0000-0002-1994-9430

Co-Author: Phoomipat Boonmapluk

E-mail: Phoomipat.bmp@gmail.com

ORCID iD: 0009-0002-8031-8926

Co-Author: Nontharit Sakda

E-mail: Nontharit.sd@gmail.com

ORCID iD: -

***Corresponding Author**

Contact: Teerapol Srichana

E-mail: teerapol.s@psu.ac.th

Early Version - Uncorrected

Affiliation: Drug Delivery System Excellence Center and Department of Pharmaceutical Technology, Faculty of Pharmaceutical Sciences, Prince of Songkla University, Songkhla, 90110, Thailand.

Running Title: CBD-Loaded HA Hydrogels: Solid-State and Rheology

Keywords: Beta-cyclodextrin inclusion complex, cannabidiol, hydrogel, polymeric micelles

Abstract:

Objective: Cannabidiol (CBD) possesses considerable anti-inflammatory and antioxidant activities; however, its pharmaceutical application is hindered by its extremely low aqueous solubility (<0.1 µg/mL). This study aimed to improve the solubility of CBD through β-cyclodextrin (β-CD) inclusion complexation combined with polymeric micelles formation and to develop a CBD-loaded hyaluronic acid (HA) hydrogel delivery system.

Material and Methods: Water-soluble CBD formulations were prepared through β-CD inclusion complexation combined with poloxamer 407-based polymeric micelle formation, followed by lyophilization. The resulting powder was subsequently incorporated into HA-based hydrogels. Solid-state characteristics were investigated using differential scanning calorimetry (DSC), Fourier transform infrared (FT-IR) spectroscopy, and powder X-ray diffraction (PXRD). Physicochemical properties, including particle size, polydispersity index (PDI), and zeta potential, were determined. Rheological properties and gelation were evaluated using a stress-controlled rheometer. In vitro CBD release was assessed using a dialysis bag diffusion method in phosphate buffer solution (PBS, pH 7.4) at 35 ± 1 °C.

Results: The aqueous solubility of CBD was markedly enhanced to 2.5 mg/mL, representing a 4,275-fold increase compared with native CBD. Solid-state characterization confirmed the transformation of crystalline CBD and the formation of a new phase. The developed hydrogels exhibited particle sizes ranging from 558.6 to 2,905.3 nm and showed a more negative zeta potential than the blank hydrogel formulation. All formulations demonstrated shear-thinning rheological behavior, whereas gelation at 15.9 °C was observed only in the blank hydrogel. In vitro release studies revealed that most formulations released CBD within 45–60 minutes.

Early Version - Uncorrected

Conclusion: The β-CD–poloxamer system effectively enhanced the aqueous solubility of CBD and enabled its stable incorporation into an HA-based hydrogel matrix. The developed formulation demonstrates promising potential as a versatile platform for CBD-based drug delivery applications.

Keywords: Beta-cyclodextrin inclusion complex, cannabidiol, hydrogel, polymeric micelles

Introduction

Cannabidiol (CBD; $C_{21}H_{30}O_2$; MW: 314.5 g/mol), the major non-psychoactive phytocannabinoid of *Cannabis sativa L.*, demonstrates significant anti-inflammatory and antioxidant properties, primarily attributed to its phenolic hydroxyl groups and hydrophobic pentyl side chain (Figure 1A)[1,2]. Due to these bioactivities, CBD has gained considerable attention for its therapeutic potential in chronic pain, autoimmune disorders, and inflammatory conditions[3,4,5]. However, its clinical application remains limited by extremely low aqueous solubility (<0.1 μg/mL)[6,7] and high lipophilicity, resulting in poor bioavailability and formulation challenges. Therefore, the development of advanced drug delivery systems is essential to improve solubility and ensure physicochemical stability for effective pharmaceutical application[8,9].

Cyclodextrins have been extensively utilized to enhance the aqueous solubility, stability, and bioavailability of poorly water-soluble drugs[10]. β-cyclodextrin (β-CD), a cyclic oligosaccharide composed of seven α-1,4-linked D-glucopyranose units, possesses a truncated cone-shaped structure with a hydrophobic internal cavity and hydrophilic external surface (Figure 1B). This unique molecular architecture enables the formation of non-covalent host–guest inclusion complexes with hydrophobic compounds, thereby improving their apparent aqueous solubility[11].

Hydrogels are three-dimensional hydrophilic polymer networks capable of absorbing large amounts of water while maintaining structural integrity, making them promising platforms for localized drug delivery[12,13]. Hyaluronic acid (HA), a biocompatible and biodegradable polysaccharide, is widely employed as a gelling agent in injectable formulations and soft-tissue applications[14]. Consequently, the development of localized delivery systems capable of modulating

Early Version - Uncorrected

the tissue microenvironment has gained increasing research interest[15]. However, the incorporation of hydrophobic compounds such as CBD into hydrophilic HA matrices remains challenging and requires effective solubilization strategies to ensure homogeneous dispersion and suitable rheological properties.

This study aimed to develop a CBD-loaded HA hydrogel system using a dual-solubilization strategy based on β-CD inclusion complexes and poloxamer 407 micelles[9,16]. The crystalline-to-amorphous transformation of CBD was investigated, together with the comprehensive rheological characterization of the hydrogel, to evaluate its suitability as an injectable delivery system. This work establishes a formulation framework for incorporating poorly water-soluble cannabinoids into hydrogel-based platforms, providing a foundation for further development of advanced therapeutic delivery systems.

Material and Methods

Materials

CBD (≥99% purity) was kindly provided by Quantum Biotech Co., Ltd. (Thailand). Hyaluronic acid (HA, 1,000 kDa), poloxamer 407 (Pluronic® F127), and β-CD were obtained from MySkinRecipes®, BASF SE, and Wacker Chemical Corp., respectively. Organic solvents and reagents were purchased from RCI Lab-scan, while other chemicals were sourced from LOBAL Chemie, KemAus, Solvay Peroxythai, and Merck KGaA. All reagents used in this study were of analytical grade.

Preparation of water-soluble CBD

Water-soluble CBD was prepared according to a previously reported method[16], with minor modifications. CBD (7.9 g) was dissolved in ethanol (78.0 g) under stirring until a clear solution was obtained. Solution A was prepared by dissolving (β-CD; 28.4 g) in water (400.0 g) at 70°C with stirring for at least 60 min, while Solution B was prepared by dispersing poloxamer 407 (9.9 g) in preheated water (70°C) under stirring until complete dissolution. Solutions A and B were combined under continuous stirring at 70°C to form a homogeneous β-CD–poloxamer micellar base. The CBD–ethanol solution was then added to the system under constant stirring, followed by thorough rinsing to ensure complete transfer. The mixture was stirred for 30 min to achieve uniform dispersion (Table 1) and subsequently freeze-dried for 42 h using an FTS Flexi-

Early Version - Uncorrected

Dry™ lyophilizer (FTS Systems, New York, NY, USA). The obtained inclusion-complex powder was collected and stored in a desiccator at 25 °C and 50.0% relative humidity, protected from light[16] (Table 1).

Table 1. The composition of water-soluble CBD[16]

Preparation of hyaluronic acid-based hydrogel

Blank hyaluronic acid (HA)-based hydrogels were prepared by dispersing HA (0.5 g) in 100 mL of phosphate buffer solution (PBS). After complete dissolution and swelling of the polymer, 125 µL of 0.02% hydrogen peroxide was added as a crosslinking agent, followed by thorough mixing at room temperature until a homogeneous hydrogel was formed (Table 2).

Chemical analysis of CBD

CBD content in the water-soluble CBD powder and CBD-loaded hydrogel was quantified using High-Performance Liquid Chromatography (HPLC) (Thermo Scientific, Massachusetts, USA) equipped with a C18 reverse-phase column (150 mm × 4.6 mm, 5 µm) maintained at 25 °C. The mobile phase consisted of acetonitrile and ultrapure water (75:25%, V/V), delivered at a flow rate of 1.0 mL/min with an injection volume of 50 µL. Detection was performed using a UV detector at 220 nm, and chromatographic data were analysed using Empower™ Software version 3.8.0.2. The analytical method was validated for specificity, limit of detection (LOD), limit of quantification (LOQ), accuracy, precision, linearity, and robustness. CBD exhibited a retention time of 3.7 min, with LOD and LOQ values of 0.25 µg/mL and 1 µg/mL, respectively.

Characterization of dried water-soluble CBD powder

Differential scanning calorimetry (DSC) Analysis

Differential scanning calorimetry (DSC) was performed to evaluate the thermal properties of CBD, poloxamer 407, β-CD, water-soluble CBD powder, and the corresponding physical mixture of CBD, β-CD, and poloxamer 407. Approximately 5-10 mg of each sample was placed in aluminum pans and analysed using a DSC 8000 instrument (PerkinElmer Inc., USA). The

Early Version - Uncorrected

samples were heated from 25 to 300 °C at a heating rate of 10 °C/min under a nitrogen atmosphere with a flow rate of 20 mL/min.

Fourier transform infrared (FT-IR Spectroscopy)

Fourier transform infrared (FT-IR) spectroscopy was conducted to analyse CBD, β-CD, poloxamer 407, water-soluble CBD powder, and the corresponding physical mixture was combined with pre-dried potassium bromide (KBr; dried at 90 °C) at a ratio of 1:10 (w/w), followed by thorough homogenisation. The mixtures were compressed at 10 bar for 30 s to form transparent pellets (2 mm in diameter). The FT-IR spectra were recorded over the wavenumber range of 4000-450 cm^{-1} using 16 scans.

Powder X-ray diffraction (PXRD) Analysis

Power X-ray diffraction (PXRD) analysis was conducted to evaluate the crystallinity and amorphous characteristics of CBD, β-CD, poloxamer 407, and water-soluble CBD powder using an Empyrean diffractometer (Malvern Panalytical, Worcestershire, UK). The measurements were performed in symmetrical reflection mode using Cu $K\alpha_1$ radiation (λ = 1.5406 Å). Diffraction patterns were recorded with a Våntec-1 line detector over a 2θ range of 3°–30° at a step size of 0.007°. The operating conditions were set at 40 kV and 40 mA with a Cu target and Ni filter, and a counting time of 0.1 s per step[17].

Hydrogel Characterization

Particle Size Distribution and Zeta Potential

The mean particle diameter and zeta potential of all CBD hydrogel formulations were determined using a nanoparticle analyzer (Malvern Zetasizer Nano ZS, ZEN3600) at 25 °C. Measurements were conducted using a 633 nm wavelength He-Ne laser with a scattering angle of 173º. The refractive indices were set at 1.540 for CBD and 1.334 for PBS. All measurements were performed in triplicate, and the results were expressed as mean ± standard deviation (SD).

Early Version - Uncorrected

Monitoring Gelation with a Rheometer

Gelation behavior was assessed by rheological analysis using an MCR 302 stress-controlled rheometer equipped with a cone–plate geometry (9 mm diameter, 2° cone angle, 0.3 mm gap). Dynamic oscillatory frequency sweep measurements were performed over a frequency range of 1-100 rad/s at a constant strain of 2.3%. The storage modulus (G') and loss modulus (G'') of the CBD hydrogel were recorded to evaluate its viscoelastic and mechanical properties.

In Vitro Drug Release Studies

The *in vitro* release of CBD from the hydrogel formulation was evaluated using a dialysis bag diffusion method. The CBD hydrogel was placed in a dialysis bag and immersed in 50 mL of PBS (pH 7.4). The system was maintained at 35 ± 1 °C under continuous stirring at 100 rpm throughout the experiment. At predetermined intervals (15, 30, 45, and 60 min), 1 mL samples were withdrawn and immediately replaced with an equal volume of fresh PBS (pH 7.4) to maintain sink conditions and constant volume. The collected samples were appropriately diluted and analyzed for CBD content using HPLC. The cumulative release profile of CBD was plotted, and the cumulative percentage release was calculated using the following equation:

$$\frac{Cumulative\ amount\ release}{Total\ drug\ load} \times 100$$

Statistical analysis

All data are presented as mean ± standard deviation (SD) from at least three independent experiments. Statistical differences among formulations were evaluated using One-way Analysis of Variance (ANOVA) followed by Tukey's post-hoc test for multiple comparisons. A p-value < 0.05 was considered statistically significant. All statistical analyses were performed using GraphPad Prism version 10.4.1.

Results

Formulation development of water-soluble CBD powder and CBD hydrogel

Water-soluble CBD powder was successfully developed to enhance the aqueous solubility of native CBD. The formulation process involved the formation of a β-CD inclusion complex at a

Early Version - Uncorrected

fixed molar ratio of 1:19 under heating at 70˚C to facilitate molecular interactions (Figure 1C). Subsequently, poloxamer 407 was incorporated to further enhance solubility through polymeric micelle formation (Figure 1D). The resulting formulation was freeze-dried, yielding a fine off-white powder at room temperature. The prepared powder exhibited an apparent aqueous solubility of 54.1 mg/mL, corresponding to a calculated CBD concentration of 427.5 µg/mL. Based on the formulation composition, in which 46.2 g of powder theoretically contained 7.9 g of CBD, the system achieved a 4,275-fold increase in solubility compared to native CBD (0.1 µg/mL). These findings confirm the substantial enhancement in CBD solubility achieved through the combined inclusion complex and micellar solubilization system.

Figure 1 Schematic representation of the formulation process and structural assembly of CBD-loaded polymeric micelles: (A) Cannabidiol (CBD); (B) β-cyclodextrin (β-CD); (C) formation of the CBD-β-CD inclusion complex through host-guest interaction; and (D) incorporation of the CBD-β-CD complex-loaded polymeric micelles, illustrating the core-shell architecture where the red region represents the hydrophobic poly(propylene oxide) (PPO) segments of the poloxamer 407, while the blue region represents the hydrophilic poly(ethylene oxide) (PEO) segments of the poloxamer 407. The hydrophobic CBD-β-CD complex is shown encapsulated within the micellar core.

Characterization of dried water-soluble CBD powder

1. DSC analysis

The thermal behavior of CBD, excipients, and the developed formulations was characterized using DSC to evaluate the physical state of the drug within the carrier system, as shown in Figure 2A.

Pure CBD: The DSC thermogram of pure CBD exhibited a sharp endothermic peak at 65.4 °C (melting range: 62.3–67.8 °C; ΔH = 56.4 J/g), corresponding to its crystalline melting point and consistent with previously reported values[6]. Pure β-CD showed an endothermic peak at 114.9 °C (ΔH = 54.1 J/g), whereas poloxamer 407 exhibited a characteristic melting peak at 54.0 °C (ΔH = 81.2 J/g).

Early Version - Uncorrected

Physical Mixture: The thermogram of the physical mixture did not display the characteristic melting peaks of CBD, β-CD, or poloxamer 407. Instead, a new endothermic peak was observed at 141.0 °C (ΔH = 86.0 J/g).

Water-Soluble CBD: The thermogram of the lyophilized water-soluble CBD powder showed the complete absence of characteristic crystalline endothermic peaks corresponding to CBD and the excipients. This result indicates the successful transformation of CBD from a crystalline to an amorphous state within the formulation system.

2. FT-IR spectroscopy

As shown in Figure 2B, FT-IR spectroscopy was employed to investigate the molecular interactions between CBD, β-CD, and poloxamer 407, and to confirm the formation of the inclusion complex. The shaded regions represent characteristic functional group vibrations corresponding to O-H stretching, C-H stretching, C=C stretching, and C-O stretching. Variations in peak intensity and peak position observed in the spectrum of the water-soluble CBD formulation suggest molecular interactions among CBD, β-CD, and poloxamer 407.

Pure CBD: The FT-IR spectrum of pure CBD exhibited characteristic peaks at 3412 cm^{-1} (O–H stretching), 3074 cm^{-1} (aromatic C=C–H stretching), and 2966–2829 cm^{-1} (aliphatic C–H stretching). Distinctive CBD peaks absent in β-CD and poloxamer 407 were observed at 1624 cm^{-1} and 1582 cm^{-1}, corresponding to alicyclic and aromatic C=C stretching vibrations, respectively. β-CD displayed a broad absorption band within the 3000–3400 cm^{-1} region attributed to O–H stretching, together with characteristic asymmetric C–O–C stretching vibrations at 1157 cm^{-1} and 1028 cm^{-1}, respectively. Poloxamer 407 showed prominent aliphatic ether C–O stretching vibrations within the 1260–1000 cm^{-1} region.

Physical Mixture: The FTIR spectrum of the physical mixture exhibited a simple superposition of the characteristic peaks of CBD, β-CD, and poloxamer 407. No significant peak shifts or changes in peak intensity were observed, suggesting the absence of substantial intermolecular interactions occurring through simple mechanical mixing at room temperature.

Water-Soluble CBD Powder: The FTIR spectrum of the water-soluble CBD powder retained the characteristic absorption bands of β-CD, while the characteristic peaks of CBD

Early Version - Uncorrected

exhibited markedly reduced intensity. Minor shifts in selected vibrational bands were also observed, suggesting intermolecular interactions between CBD and the carrier components.

3. PXRD analysis

Crystallinity of CBD: Consistent with previous reports[18], pure CBD exhibited characteristic crystalline diffraction peaks at 2θ values of 9.7, 11.7, 13.1, 15.1, 16.6, 17.4, 18.8, 21.6, 22.2, and 22.7, confirming its highly crystalline nature. β-CD similarly displayed distinct crystalline reflections at 2θ values of 9.0, 10.7, 12.5, 15.4, 18.9, 20.7, 22.7, 27.0, 34.9, and 45.2[18]. The PXRD pattern of poloxamer 407 exhibited two broad diffraction peaks with intense reflections at 2θ values of 19.1° and 23.3°, characteristic of its semi-crystalline poly (ethylene oxide) segments.

Water-Soluble CBD Powder: As shown in Figure 2C, the PXRD pattern of the water-soluble CBD powder demonstrated the disappearance of the characteristic diffraction peaks of crystalline CBD, particularly at 2θ values of 9.7˚, 11.7˚, 13.1˚, and 15.1˚. Concurrently, new diffraction reflections emerged at 5.9˚, 6.7˚, 19.2˚, 20.1˚, and 23.6˚ (2θ), indicating the formation of a distinct solid-state phase and confirming the successful incorporation of CBD within the β-CD/poloxamer 407 system.

Figure 2 Physicochemical characterization of the water-soluble CBD powder compared with the individual components and physical mixture: **(A)** Differential Scanning Calorimetry (DSC) thermograms recorded from 40°C to 170°C at a heating rate of 10°C/min; **(B)** Fourier-Transform Infrared (FT-IR) spectra acquired over the wavenumber range of 4000–500 cm^{-1}; and **(C)** powder X-ray diffraction (PXRD) pattern of CBD[18], β-CD[18], poloxamer 407, and the water-soluble CBD powder.

Based on the FT-IR spectral changes and the disappearance of crystalline peaks observed in the DSC analysis, Figure 3 illustrates a proposed inclusion configuration of CBD within the β-CD cavity. The hydrophobic moiety of CBD is likely accommodated within the hydrophobic cavity of β-CD, while the hydroxyl groups of β-CD remain oriented toward the aqueous environment. This host–guest interaction may contribute to the enhanced aqueous solubility of CBD. The proposed molecular arrangements may also contribute to the improved stability of CBD within the dual-solubilization system.

Early Version - Uncorrected

Figure 3 Proposed schematic illustration of the potential structural configurations of the CBD, β-CD, and poloxamer 407 assembly: **(A)** Direct encapsulation of free CBD within the hydrophobic poly(propylene oxide) (PPO) core of the poloxamer 407 micelle; **(B)** encapsulation of the CBD-β-CD inclusion complex within the micellar core, facilitated by the hydrophobic nature of the complex; and **(C)** association of the CBD-β-CD inclusion complex with the hydrophilic poly(ethylene oxide) (PEO) shell through hydrogen bonding or steric entrapment. The red and blue regions represent the hydrophobic and hydrophilic segments of poloxamer 407, respectively. The yellow sphere denotes CBD, while the purple truncated cone represents β-CD.

Physical properties of CBD hydrogel

The physicochemical properties of the developed CBD hydrogels, including particle size, polydispersity index (PDI), and zeta potential, were evaluated. For hydrogel-based delivery systems, acceptable physicochemical characteristics generally include particle sizes ≤500 nm, polydispersity index (PDI) values ≤0.5, zeta potential magnitudes >30 mV, and physiological pH ranges of 6.5–7.4[19]. The blank hydrogel (CBD-G1) exhibited a Z-average diameter of 975.8±78.46 nm with a PDI of 0.47 ± 0.02. Following incorporation of the water-soluble CBD powder, particle sizes varied among the formulations, ranging from 558.6 ± 84.91 nm (CBD-G5) to 2,905.3±352.19 nm (CBD-G3). The PDI values of the CBD-loaded formulations ranged from 0.3 (CBD-G4) to 0.6 (CBD-G5). The zeta potential of the blank hydrogel was −18.7 ± 0.71 mV, whereas formulations containing water-soluble CBD exhibited more negative values, including −34.1 ± 0.62 mV observed for CBD-G2 and −32.9 ± 1.61 mV for CBD-G5. Quantitative analysis of the water-soluble CBD powder demonstrated a CBD recovery of 90.8 ± 6.2% relative to the theoretical amount.

The similar zeta potential values observed among the formulations, despite variations in CBD loading, may be attributed to the structural characteristics of the polymeric micelles. In such systems, hydrophobic drugs are predominantly encapsulated within the micellar core, while the hydrophilic drugs are predominantly encapsulated within the micellar core, and the hydrophilic outer shell primarily governs the interfacial properties of the formulation[20, 21].

As the surface charge is primarily governed by the hydrophilic corona and can only be significantly altered through surface modification[22], variations in the amount of encapsulated

Early Version - Uncorrected

CBD do not substantially affect the zeta potential. This explains why formulations with different CBD loadings exhibited comparable surface charge values.

Table 2 Physical properties of CBD hydrogel formulations (mean ± SD, n=3)

Characterization of CBD hydrogel

Gelation behavior

The gelation behavior of the CBD hydrogels was evaluated by measuring the storage modulus (G′) and loss modulus (G″) as a function of temperature. The sol-gel transition temperature was determined from the crossover point of G′ and G″, corresponding to the transition from a sol state to a gel state[23]. As shown in Figure 4A, temperature sweep measurements were conducted over the range of 7-60 °C. Among the tested formulations, only CBD-G1 exhibited a crossover point between G′ and G″, indicating a sol–gel transition at 15.9 °C. In contrast, all CBD-loaded formulations (CBD-G2 to CBD-G5) exhibited no crossover point within the investigated temperature range, with G" remaining higher than G' throughout the heating process.

Figure 4 Temperature-dependent rheological profiles of the CBD-loaded hydrogel formulations. The storage modulus (G′) and loss modulus (G″) were measured as a function of temperature (7°C - 60°C) for (A) CBD-G1, (B) CBD-G2, (C) CBD-G3, (D) CBD-G4, and (E) CBD-G5. Solid lines represent G′ (elastic behavior), while dashed lines represent G" (viscous behavior). Measurements were performed using an MCR 302 stress-controlled rheometer equipped with a cone–plate geometry (9 mm diameter, 2°cone angle, and 0.3 mm gap) at a constant strain of 2.3%. The relative magnitudes and crossover behavior of G' and G" were used to characterize the viscoelastic properties and thermal response of the hydrogel systems.

3.4.2. Rheological Behavior and Gelation Analysis

Rheological analysis was conducted to evaluate the sol-gel transition and flow behavior of the developed formulations. Temperature sweep measurements revealed that only the blank hydrogel (CBD-G1) exhibited a defined gelation temperature at 15.9 °C, as evidenced by the

Early Version - Uncorrected

crossover of storage modulus (G′) and loss modulus (G″) (Figure 5). In contrast, CBD-loaded formulations (CBD-G2 to CBD-G5) did not demonstrate any G′/ G″ crossover within the tested temperature range, with G″ remaining higher than G′ throughout the analysis. All formulations exhibited shear-thinning behavior, characterized by a decrease in apparent viscosity with an increasing shear rate (0.1 to 100^{-1}). Additionally, viscosity values at 25°C (Figure 5A) were slightly higher than those measured at 37°C (Figure 5B).

Figure 5 Rheological characterization of CBD hydrogel formulations under steady shear at 25°C(A) and 37°C(B). The plots illustrate apparent viscosity (η) versus shear rate (0.1 to 100 s^{-1}) for CBD-G1 to CBD-G5. Measurements were obtained using an MCR 302 rheometer with a cone–plate geometry (9 mm diameter, 2° cone angle, 0.3 mm gap).

3.5 In vitro CBD release from the CBD hydrogel

The *in vitro* release profile of CBD from hydrogel formulations was evaluated using a dialysis bag method in PBS (pH 7.4) at 35 ± 1 °C over 60 min (Figure 6). All formulations exhibited a rapid initial burst release of CBD. At 15 min, CBD-G2 achieved complete release ~~of~~ (100 ± 3%), while CBD-G3, CBD-G4, and CBD-G5 showed release values of 89.2 ± 24.0%, 86.9 ± 26.0%, and 91.5 ± 3%, respectively. At 45 min, release from all formulations approached complete levels. After 60 min, CBD-G2, CBD-G3, and CBD-G5 reached approximately 100.0 ± 31.0%, 100.0 ± 24.0%, and 100.0 ± 25.0%, respectively, whereas CBD-G4 showed a slightly higher value of 112.0 ± 26.0%. Overall, all formulations released most of the encapsulated CBD within 45–60 min, with no statistically significant differences observed ($P > 0.05$).

Figure 6 In vitro release profiles of CBD-loaded hydrogel formulations determined using the dialysis bag method in phosphate-buffered saline (PBS, pH 7.4) at 35±1°C for 60 minutes. Formulations CBD-G2, CBD-G3, CBD-G4, and CBD-G5 are represented by different symbols. Values are expressed as mean ± SD (n=6).

Discussion

The solid-state characterization of the developed water-soluble CBD powder demonstrated substantial structural modification relative to native CBD. The complete disappearance of the characteristic CBD melting endotherm in the DSC thermogram, together with the reduced intensity

Early Version - Uncorrected

of FTIR absorption bands, indicates successful molecular dispersion within the carrier matrix. Such a transformation from a crystalline to an amorphous or less ordered state is commonly regarded as evidence of successful complexation[7,9]. Furthermore, the appearance of new PXRD reflections distinct from those of the parent components confirms the formation of a new supramolecular solid-state phase rather than a simple physical mixture. Similar findings have been widely reported in cyclodextrin-based delivery systems, where inclusion complex formation disrupts the crystalline lattice of hydrophobic compounds, thereby enhancing solubility and modifying thermal properties.

Particle size differences among the formulations may result from complex interactions between CBD, polymeric micelles, and the hydrogel network. Elevated CBD content could increase hydrophobic core loading, thereby promoting micellar enlargement or aggregation. Simultaneously, interactions between the micellar structures and the hyaluronic acid matrix may favor the formation of larger supramolecular complexes at higher concentrations. In addition, the concentration- and temperature-sensitive self-assembly behavior of poloxamer 407 likely contributes to the observed variations in particle size distribution[20,21].

These combined effects likely account for the observed variability in particle size among the formulations, highlighting the complex interplay between drug loading, micellar organization, and hydrogel network structure. Similar phenomena have been reported in polymeric micelle–hydrogel systems, where particle size is strongly influenced by both hydrophobic core loading and intermolecular polymer–polymer interactions.

The absence of a distinct sol–gel transition in CBD-loaded formulations suggests that incorporation of the CBD-β-CD inclusion complex disrupted the thermal gelation behavior of the Poloxamer 407/HA matrix. This effect is likely associated with structural reorganization of the micellar networks following incorporation of the bulky supramolecular complex. Nevertheless, all formulations retained pronounced shear-thinning (pseudoplastic) behavior—a desirable characteristic for injectable delivery systems[13, 15].

The observed rheological behavior indicates that incorporation of the CBD–β-CD inclusion complex altered the internal organization of the hydrogel matrix. The lack of a clear sol–gel transition in CBD-loaded formulations suggests interference with the micellar interactions responsible for thermally induced gelation. However, all formulations maintained shear-thinning

Early Version - Uncorrected

characteristics, an essential property for injectable systems that facilitates flow during injection and structural recovery after administration.

The rapid release profile observed for all formulations is consistent with diffusion-controlled transport of CBD from the hydrogel matrix. The amorphous nature of CBD and its incorporation within micellar domains likely facilitate immediate interaction with the aqueous medium, thereby enhancing dissolution. In addition, the hydrophilic hyaluronic acid matrix promotes water uptake and penetration, further accelerating drug diffusion into the release medium. This initial burst release may be beneficial for applications requiring rapid therapeutic onset; however, further formulation optimization would be necessary to achieve sustained release behavior.

Conclusion

This study successfully developed a CBD-loaded hyaluronic acid hydrogel system using a dual-solubilization approach. The combined effects of β-cyclodextrin inclusion complexation and Poloxamer 407 were a 4,275-fold enhancement in the aqueous solubility of CBD. Solid-state analyses (DSC, FT-IR, and PXRD) confirmed the molecular transformation of crystalline CBD into a stable amorphous inclusion complex within the carrier matrix. Rheological evaluation demonstrated that although incorporation of the CBD complex-altered the thermogelling behavior of the system, all formulations retained desirable shear-thinning (pseudoplastic) properties suitable for injectable administration. In addition, the hydrogel formulations efficiently released encapsulated CBD under physiological conditions within 45–60 minutes. Collectively, these findings highlight the potential of this formulation platform to deliver poorly water-soluble cannabinoids via biocompatible hydrogel systems for advanced therapeutic applications.

Acknowledgment

The authors gratefully acknowledge Mr. Ekawat Thawitong for technical support and assistance. The authors also thank the Drug Delivery System Excellence Center (DDSEC), Faculty of Pharmaceutical Sciences, Prince of Songkhla University, for providing laboratory facilities.

Early Version - Uncorrected

Funding sources

This research was supported by Prince of Songkhla University, Talent Utilization Type 2 (grant number TU2-08/2564).

Conflict of interest

The authors declare no competing interests.

References

1. Martinez Naya N, Kelly J, Corna G, Golino M, Abbate A, Toldo S. Molecular and Cellular Mechanisms of Action of Cannabidiol. Molecules. 2023 Aug 9;28(16):5980. doi: 10.3390/molecules28165980. PMID: 37630232; PMCID: PMC10458707.
2. Patel P, Curry S. Cannabidiol (CBD) in Clinical Care. [Updated 2024 May 7]. In: StatPearls [Internet]. Treasure Island (FL): StatPearls Publishing; 2026 Jan-. Available from: https://www.ncbi.nlm.nih.gov/books/NBK556048/
3. Martinez Naya N, Kelly J, Corna G, Golino M, Polizio AH, Abbate A, et al. An Overview of Cannabidiol as a Multifunctional Drug: Pharmacokinetics and Cellular Effects. Molecules. 2024 Jan 18;29(2):473. doi: 10.3390/molecules29020473. PMID: 38257386; PMCID: PMC10818442.
4. Ruth G, Zhannah Y, and Lumír HO. The anti-inflammatory properties of terpenoids from cannabis. Cannabis Cannabinoid Res. 2018; 3(1):282-90. https://doi.org/10.1089/can.2018.0014
5. Atalay S, Iwona JK, Elzbieta S. Antioxidative and anti-inflammatory properties of cannabidiol. Antioxidants. 2019; 9(1), 21. https://doi.org/10.3390/antiox9010021
6. Stinchcomb AL, Valiveti S, Hammell DC, Ramsey DR. Human skin permeation of Δ^8-tetrahydrocannabinol, cannabidiol and cannabinol. J Pharm Pharmacol. 2004; 56(3): 291-7. https://doi.org/10.1211/0022357022791
7. Li H, Chang S, Tanran C, You Y, Wang X, Liwei W, et al. Inclusion complexes of cannabidiol with β-cyclodextrin and its derivative: physicochemical properties, water solubility, and antioxidant activity. J Mol Liq. 2021; 334:116070. https://doi.org/10.1016/j.molliq.2021.116070

Early Version - Uncorrected

8. ElSohly MA, Slade D. Chemical constituents of marijuana: the complex mixture of natural cannabinoids. Life sciences, 2005; 78.5: 539-548. https://doi.org/10.1016/j.lfs.2005.09.011
9. Triamchaisri N, Toochinda P, Lawtrakul L. Structural investigation of beta-cyclodextrin complexes with cannabidiol and delta-9-tetrahydrocannabinol in 1:1 and 2:1 Host-Guest Stoichiometry: Molecular Docking and Density Functional Calculations. Int J Mol Sci. 2023;24(2):1525. https://doi.org/10.3390/ijms24021525
10. Esteso MA, Romero CM. Cyclodextrins: Properties and Applications. Int J Mol Sci. 2024 Apr 21;25(8):4547. doi: 10.3390/ijms25084547. PMID: 38674132; PMCID: PMC11050477.
11. National Center for Biotechnology Information. PubChem Compound Summary for CID 444041, beta-Cyclodextrin. https://pubchem.ncbi.nlm.nih.gov/compound/beta-Cyclodextrin. Accessed Mar. 13, 2026.
12. Ahmed EM. Hydrogel: preparation, characterization, and applications: a review. J Adv Res. 2015;6(2):105-21. https://doi.org/10.1016/j.jare.2013.07.006
13. Correa S, Grosskopf AK, Hernandez HL, Chan D, Yu AC, Stapleton LM, et al. Translational applications of hydrogels. Chemical Reviews. 2021;121(18):11385-457.
14. Huang G, Huang H. Application of hyaluronic acid as carriers in drug delivery. Drug Delivery. 2018; 25(1), 766–772. https://doi.org/10.1080/10717544.2018.1450910
15. Li J, Mooney DJ. Designing hydrogels for controlled drug delivery. Nat Rev Mater. 2016; 1(12):16071. https://doi:10.1038/natrevmats.2016.71
16. Changsan N, Sawatdee S, Suedee R, Chunhachaichana C, Srichana T. Aqueous cannabidiol β-cyclodextrin complexed polymeric micelle nasal spray to attenuate in vitro and ex vivo SARS-CoV-2-induced cytokine storms. Int J Pharm. 2023; 640:123035. https://doi.org/10.1016/j.ijpharm.2023.123035
17. Vlad RA, Sovany T, Kristo K, Ibrahim Y, Ciurba A, Aigner Z, et al. Structural and thermal analysis of cannabidiol orodispersible formulations. Farmacia. 2021; 69(3):426-33. https://doi.org/10.31925/farmacia.2021.3.5
18. Sangsanoh P, Chaiarwut S, Choipang C, Niyompanich J, Suwantong O, et al. Cannabidiol/β-Cyclodextrin Inclusion Complex-Loaded Poly(Vinyl Alcohol) Semi-solid Hydrogels for Potential Use in Wound Management. J Polym Environ 2023; 31, 3982–3997. https://doi.org/10.1007/s10924-023-02845-7

Early Version - Uncorrected

19. Alonso JM, Andrade del OJ, Perez GR, Saez MV. Injectable Hydrogels: From Laboratory to Industrialization. Polymers. 2021; 13(4), 650. https://doi.org/10.3390/polym13040650
20. Torchilin, VP. Structure and design of polymeric surfactant-based drug delivery systems. Journal of controlled release. 2001; 137-172. https://doi.org/10.1016/S0168-3659(01)00299-1
21. Jassim ZE, A. Rajab N. An Insight into Polymeric Micelles Preparation Methods and Applications as Drug Delivery Approach: A Review. International Journal of Pharmaceutical Investigation. 2025;15(3):849-857. doi: 10.5530/ijpi.20250305
22. Guzmán RA, Sablón CM, Rodríguez TC, Malessy MJA, Fuentes G, Cruz LJ. Smart Polymeric Micelles for Anticancer Hydrophobic Drugs. Cancers (Basel). 2022 Dec 20;15(1):4. https://doi.org/10.3390/cancers15010004
23. Yilmazer S, Schwaller D, Mésini PJ. Beyond Sol-Gel: molecular gels with different transitions. Gels. 2023; 9(4):273. https://doi.org/10.3390/gels9040273

Early Version - Uncorrected

Table 1 The composition of water-soluble CBD[16]

Ingredients	Amount (1kg)	Function
CBD	7.9 g	Active ingredient
β-CD	28.4 g	Encapsulate
Poloxamer 407	9.9 g	Surfactant
Ethanol	78.0 g	Solvent
Water	875.8 g	Solvent

Table 2 Physical properties of CBD hydrogel formulations (mean ± SD, n=3)

Formulation	CBD (mg%)	Water-soluble CBD (mg%)	Particle size (Z-average, nm)	PDI	Zeta potential (mV)
CBD-G1	-	-	975.8 ±78.46	0.47 ± 0.02	−18.7 ± 0.71
CBD-G2	3.1	18.3	1523.0 ± 102.32	0.39 ± 0.03	−34.1 ± 0.62
CBD-G3	6.3	36.5	2905.3 ±352.19	0.36 ± 0.04	−27.4 ± 0.74
CBD-G4	12.5	73.1	1924.0 ±154.86	0.29 ± 0.01	−27.3 ± 1.73
CBD-G5	25.0	146.2	558.6 ±84.91	0.62 ± 0.02	−32.9 ± 1.61

Early Version - Uncorrected

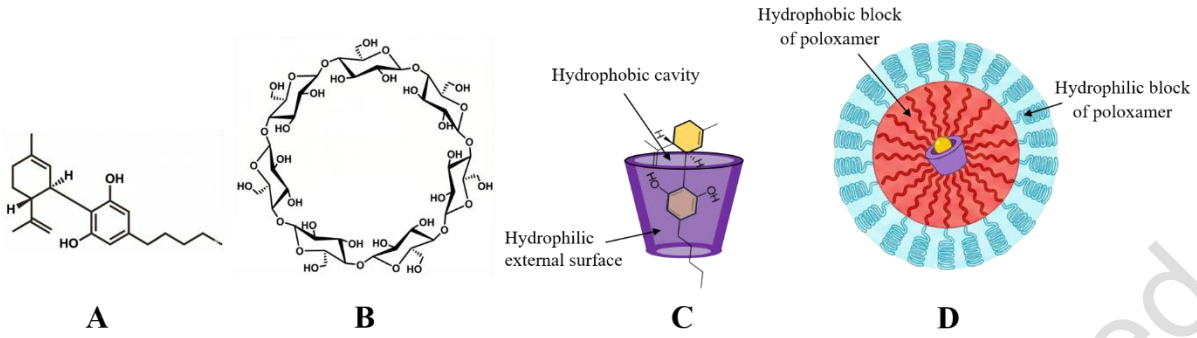


Figure 1 Schematic representation of the formulation process and structural assembly of CBD-loaded polymeric micelles: (A) Cannabidiol (CBD); (B) β-cyclodextrin (β-CD); (C) formation of the CBD-β-CD inclusion complex through host-guest interaction; and (D) incorporation of the CBD-β-CD complex-loaded polymeric micelles, illustrating the core-shell architecture where the red region represents the hydrophobic poly(propylene oxide) (PPO) segments of the poloxamer 407, while the blue region represents the hydrophilic poly(ethylene oxide) (PEO) segments of the poloxamer 407. The hydrophobic CBD-β-CD complex is shown encapsulated within the micellar core.

Early Version - Uncorrected

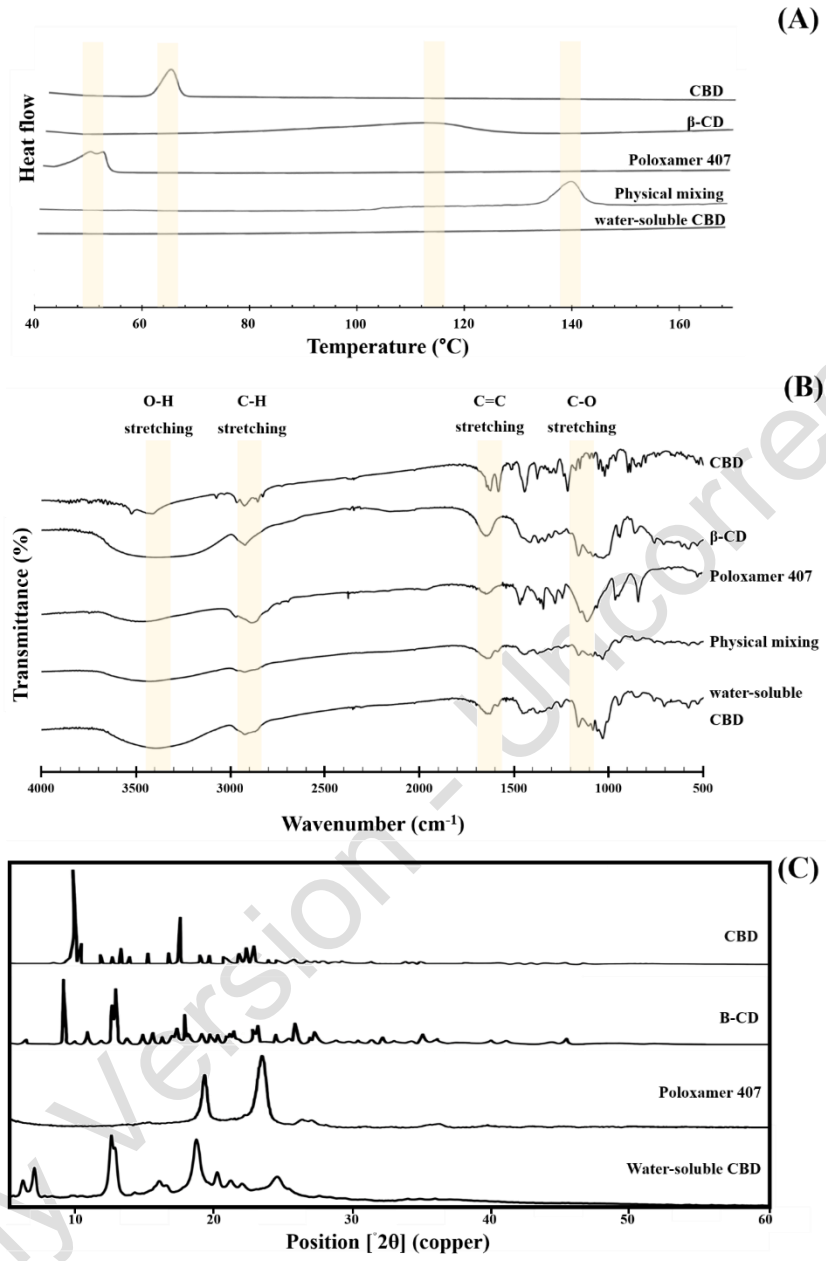


Figure 2 Physicochemical characterization of the water-soluble CBD powder compared with the individual components and physical mixture: **(A)** Differential Scanning Calorimetry (DSC) thermograms recorded from 40°C to 170°C at a heating rate of 10°C/min; **(B)** Fourier-Transform Infrared (FT-IR) spectra acquired over the wavenumber range of 4000–500 cm^{-1}; and **(C)** powder X-ray diffraction (PXRD) pattern of CBD[18], β-CD[18], poloxamer 407, and the water-soluble CBD powder.

Early Version - Uncorrected

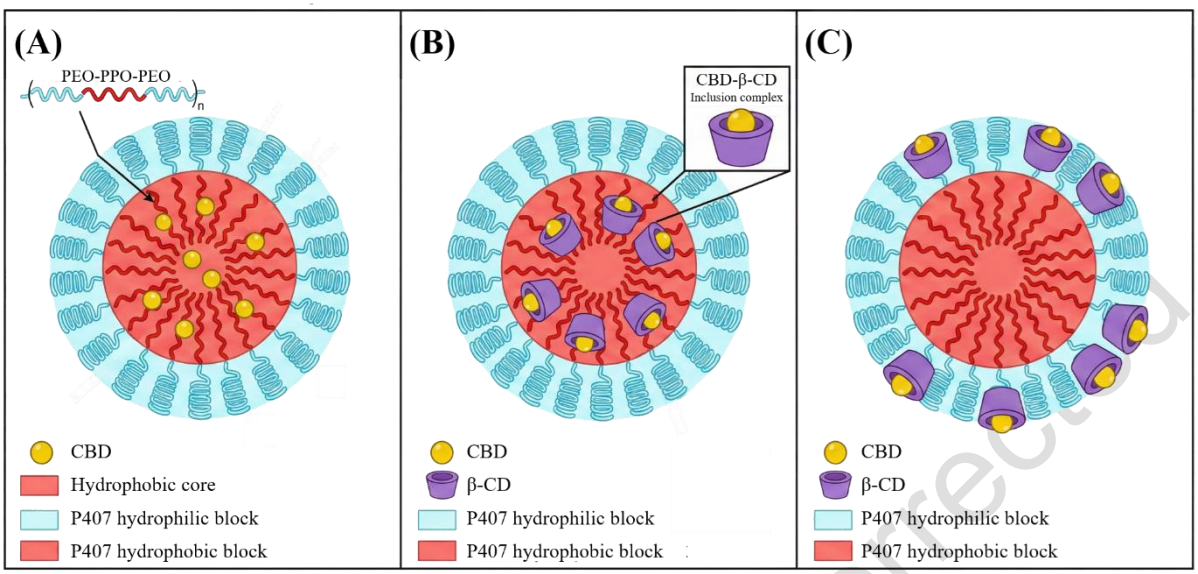


Figure 3 Proposed schematic illustration of the potential structural configurations of the CBD, β-CD, and poloxamer 407 assembly: **(A)** Direct encapsulation of free CBD within the hydrophobic poly(propylene oxide) (PPO) core of the poloxamer 407 micelle; **(B)** encapsulation of the CBD-β-CD inclusion complex within the micellar core, facilitated by the hydrophobic nature of the complex; and **(C)** association of the CBD-β-CD inclusion complex with the hydrophilic poly(ethylene oxide) (PEO) shell through hydrogen bonding or steric entrapment. The red and blue regions represent the hydrophobic and hydrophilic segments of poloxamer 407, respectively. The yellow sphere denotes CBD, while the purple truncated cone represents β-CD.

Early Version - Uncorrected

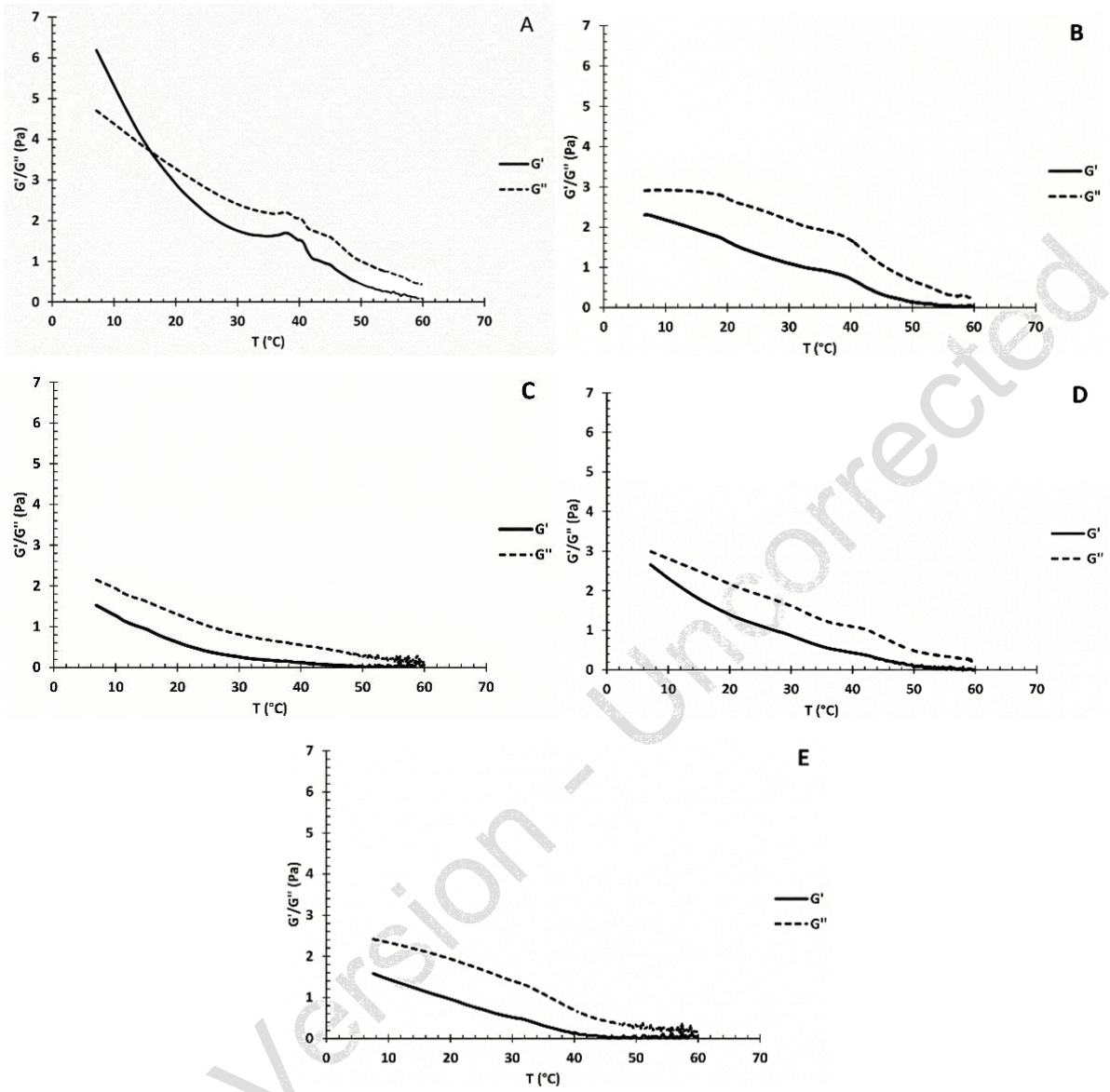


Figure 4 Temperature-dependent rheological profiles of the CBD-loaded hydrogel formulations. The storage modulus (G′) and loss modulus (G′′) were measured as a function of temperature (7°C - 60°C) for (A) CBD-G1, (B) CBD-G2, (C) CBD-G3, (D) CBD-G4, and (E) CBD-G5. Solid lines represent G′ (elastic behavior), while dashed lines represent G'' (viscous behavior). Measurements were performed using an MCR 302 stress-controlled rheometer equipped with a cone–plate geometry (9 mm diameter, 2°cone angle, and 0.3 mm gap) at a constant strain of 2.3%. The relative magnitudes and crossover behavior of G' and G'' were used to characterize the viscoelastic properties and thermal response of the hydrogel systems.

Early Version - Uncorrected

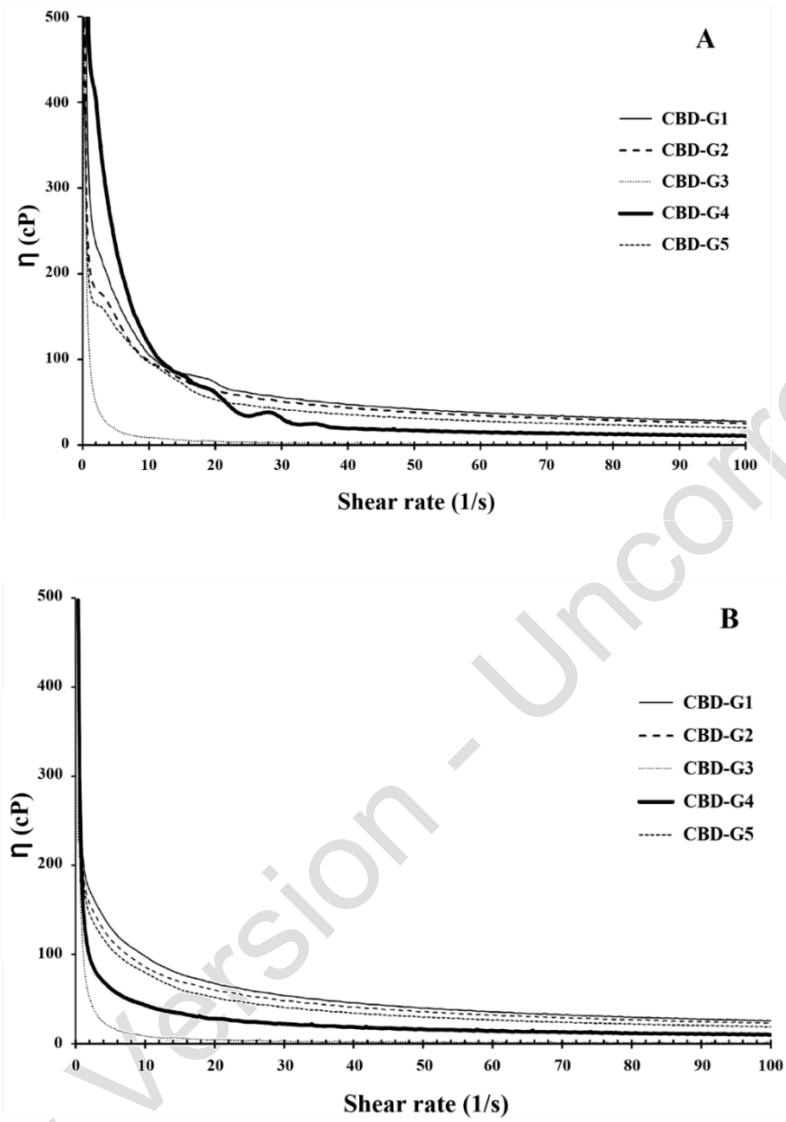


Figure 5 Rheological characterization of CBD hydrogel formulations under steady shear at 25°C(A) and 37°C(B). The plots illustrate apparent viscosity (η) versus shear rate (0.1 to 100 s^{-1}) for CBD-G1 to CBD-G5. Measurements were obtained using an MCR 302 rheometer with a cone–plate geometry (9 mm diameter, 2° cone angle, 0.3 mm gap).

Early Version - Uncorrected

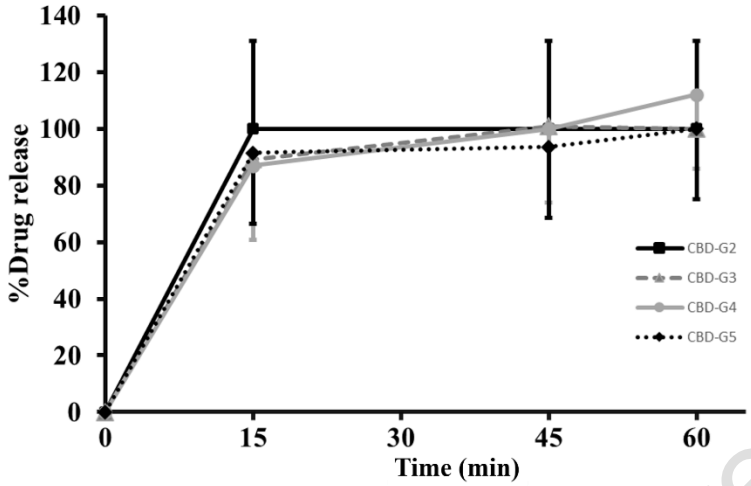


Figure 6 In vitro release profiles of CBD-loaded hydrogel formulations determined using the dialysis bag method in phosphate-buffered saline (PBS, pH 7.4) at 35±1°C for 60 minutes. Formulations CBD-G2, CBD-G3, CBD-G4, and CBD-G5 are represented by different symbols. Values are expressed as mean ± SD (n=6).

Early Version - Uncorrected